

# MULTI-SCALE IMAGE DENOISING WHILE PRESERVING EDGES IN SPARSE DOMAIN

*Srimanta Mandal, Seema Kumari, Arnav Bhavsar, and Anil Kumar Sao*

School of Computing and Electrical Engineering  
Indian Institute of Technology Mandi, India

{srimanta\_mandal, seema\_kumari}@students.iitmandi.ac.in, {arnav, anil}@iitmandi.ac.in

## ABSTRACT

Image denoising is a classical and fundamental problem in image processing community. An important challenge in image denoising is to preserve image details while removing noise. However, most of the approaches depend on smoothness assumption of natural images to produce results with smeared edges, hence, degrading the quality. To address this concern, we propose two constraints to better preserve the edges while denoising the image via the sparse representation framework. The first constraint attempts to preserve the edges at the coarser scales of the image as the level of noise drop dramatically at coarser scales. Different levels of scales are considered to account different strength of noise. The second constraint prevents transitional smoothing by preserving the edges of intermediate image estimates across iterations. Experimental results demonstrate the ability of the proposed approach in removing noise while preserving edges in comparison to the state-of-the art approaches.

**Index Terms**— Image denoising, Down-sampling, Edge-preservation, Sparse-representation.

## 1. INTRODUCTION

Ever-increasing demand of visual information often requires high quality images of scenes. However, sensor imperfection, poor illumination, communication errors etc. may introduce noise in the captured image. Thus, it is necessary to restore the noisy image. If noise is assumed to be additive then the following mathematical model can be used:

$$\mathbf{y} = \mathbf{x} + \mathbf{n}, \quad (1)$$

where,  $\mathbf{x} \in \mathcal{R}^M$  is the original scene which is degraded by additive zero mean white Gaussian noise  $\mathbf{n} \in \mathcal{R}^M$  with standard deviation  $\sigma$  to produce the degraded (noisy) image  $\mathbf{y} \in \mathcal{R}^M$ . Image denoising aims to recover an estimate of  $\mathbf{x}$  from  $\mathbf{y}$ , which is as close as possible to the original image. It is an example of classical inverse problem and can be solved by regularizing the same with some prior knowledge as

$$\hat{\mathbf{x}} = \arg \min_{\mathbf{x}} \left\{ \|\mathbf{y} - \mathbf{x}\|_2^2 + \lambda \mathbf{R}(\mathbf{x}) \right\}, \quad (2)$$

where,  $\mathbf{R}(\mathbf{x})$  is regularization term used to incorporate prior knowledge.

Most of the image denoising algorithms are centered around modeling the prior information  $\mathbf{R}(\mathbf{x})$  implicitly or explicitly. Majority of the approaches perform denoising based on the assumption that the natural image contains mostly smoother regions. Implicitly, the smoothness prior is incorporated by smoothing the entire image by means of convolving the noisy image with Gaussian kernel [1] or by smoothing within a boundary rather than across boundary [2]. On the other hand, prior information is incorporated explicitly as  $\mathbf{R}(\mathbf{x})$  in the form of total-variation (TV) [3], Gaussian mixture model (GMM) [4], non-local self similarity (NLSS) [1, 5–7], sparsity [8–10] etc. While most of the mentioned approaches yield good results, there is always a trade-off between suppression of noise and smearing of edges, which is perceptually important aspect of any image.

In this paper, we address the problem of image denoising in a novel representation of the sparse coding framework, by considering two effects of multiscale processing and edginess representation [11] on noise reduction and edge preservation. We initialize our model with the Nonlocally Centralized Sparse Representation (NCSR) approach [10], over and above which, we incorporate constraints to take into account the above mentioned effects.

The first constraint attempts to minimize the difference between the edges of the denoised image (potential solution) and the noisy image at coarser scale. It is based on the observation, as well as supported in literature [12], that levels of noise drop significantly at coarser image scales and strong edges are less affected. Thus, it is logical to make edges of the noisy image consistent with the denoised one at the coarser scale. The coarser image scale is generated by blurring and subsampling the image. However, it is difficult to come up with a suitable scale factor for down-sampling because while the level of noise is suppressed better for larger down-sampling factor, there is some loss of information. Hence, the proposed approach considers edge preservation at multiple down-sampling factors.

The second constraint attempts to preserve the edges of denoised image over different iterations. It has been observed that denoising algorithm has to iterate few times to reduce

the level of noise efficiently. As the iterations progress the level of noise comes down but edges also get blurred. Hence, a constraint is added to preserve the edges of the intermediate denoised image at each iteration. It can be seen as a step to mitigate the transitional smoothing. The robustness of the proposed approach is demonstrated by testing the performance under different strength of noise. Moreover, the proposed constraints can be added with any existing image denoising approach. In this paper, the results are demonstrated with image denoising using the framework of sparse coding.

Hence, the contribution of the paper can be summarized as: i) As the level of noise is reduced significantly at coarser scale of noisy image, a constraint is proposed to preserve the edges of down-sampled denoised image. ii) In order to deal with different amount of noise, the edge preservation is carried out for different scales. iii) The transitional smoothing is mitigated by preserving edges of intermediate denoised image in iterative based denoising approach.

The structure of the remaining paper is depicted as follows: Section 2 gives a brief background about denoising an image via sparse representation by eliminating sparse coding noise, employed in this work. The edges of the denoised image are preserved using two constraints, and are described in Section 3. The robustness of the proposed approach is manifested in Section 4 through experimental results and the summary is given in Section 5.

## 2. IMAGE DENOISING IN SPARSE DOMAIN

Although, our approach can be embedded in any of the iterative denoising algorithms, we have used sparse representation framework because of its ability to perform better [13–18]. The underlying concept is that an image can be sparsely represented with the help of a dictionary matrix i.e.  $\mathbf{x} = \mathbf{A}\mathbf{c}$ , where  $\mathbf{c}$  is the sparse coefficient vector that has to be achieved with the help of the dictionary matrix  $\mathbf{A}$  as

$$\hat{\mathbf{c}} = \arg \min_{\mathbf{c}} \left\{ \|\mathbf{y} - \mathbf{A}\mathbf{c}\|_2^2 + \lambda \|\mathbf{c}\|_1 \right\}. \quad (3)$$

Once,  $\hat{\mathbf{c}}$  is computed, the image  $\mathbf{x}$  can be restored as  $\hat{\mathbf{x}} = \mathbf{A}\hat{\mathbf{c}}$ . Here, the denoising of images works based on the assumption that the noisy image as well as the unknown clean image share the same sparse coefficient vector. Nevertheless, the assumption may not be logical as sparse coding the clean image or its noisy version may not produce the same coefficient vector. Let's  $\hat{\mathbf{c}}_{\mathbf{x}}$  and  $\hat{\mathbf{c}}_{\mathbf{y}}$  be the coefficient vectors for clean and the noisy version of the image, respectively. One requires to minimize the difference between  $\hat{\mathbf{c}}_{\mathbf{x}}$  and  $\hat{\mathbf{c}}_{\mathbf{y}}$ , which is termed as sparse coding noise in literature [10]. In practice  $\hat{\mathbf{c}}_{\mathbf{x}}$ <sup>1</sup> is not available and approximated using  $\psi_i$ , which is sparse coefficient vector computed from non-local mean of

<sup>1</sup> $\hat{\mathbf{c}}_{\mathbf{x}_i}$  is the sparse coefficient vector of patch  $\mathbf{x}_i$ , which is the  $i^{\text{th}}$  patch extracted from the image  $\mathbf{x}$  as  $\mathbf{x}_i = \mathbf{P}_i\mathbf{x}$ .

similar patches. Thus, the sparse coding noise can be reduced as

$$\hat{\mathbf{c}}_{\mathbf{y}} = \arg \min_{\mathbf{c}} \left\{ \|\mathbf{y} - \mathbf{A}\mathbf{c}\|_2^2 + \lambda \sum_i \|\mathbf{c}_i - \psi_i\|_1 \right\}. \quad (4)$$

The resultant  $\hat{\mathbf{c}}_{\mathbf{y}}$  is now very close to the sparse vector of unknown image  $\mathbf{x}$ , and can be multiplied with the dictionary matrix to achieve an approximation of denoised image as  $\hat{\mathbf{x}} = \mathbf{A}\hat{\mathbf{c}}_{\mathbf{y}}$ .

In this work, we have used the same dictionary learning strategy as mentioned in [10], where patches are extracted from the input image, and cluster them into  $K$  groups using  $K$ -means clustering method. The reason being that different clusters contain different variations of image structures, and can effectively represent natural image than an over-complete dictionary. Each of the  $K$  clusters contains similar patches, hence, we do not have to learn over-complete dictionaries for each of them. Instead, a compact dictionary is learned for each of the cluster using principal component analysis (PCA) approach. For decades, PCA has been used to de-correlate or to reduce dimension of signal, and is very successful in image restoration work [10, 14, 15]. Hence, PCA can be effectively used to learn compact dictionary. Moreover, a compact dictionary will reduce computational cost, in comparison to an over-complete dictionary.

## 3. PROPOSED CONSTRAINTS FOR EDGE PRESERVATION

In the following sub-sections, we discuss the proposed two constraints for preserving edges in sparse coding based image denoising algorithm. Here, both the constraints are incorporated within each iteration of image denoising algorithm.

### 3.1. Preserving edges at coarser scales

Here, we attempt to preserve the edginess feature [11], which is the magnitude of gradient of image (computation will be explained later), between the noisy image and the denoised image at coarser scale. The reason for using down-sampled or coarser scale of image instead of noisy image at the same scale is that the coarser version of the noisy image contains lesser noise [12] and can produce a less noisy edges as compared to the noisy image. This is, possibly, because of the fact that down-sampling operation involves some filtering (smoothing) of the image, and hence a reduction in noise, which is typically uncorrelated.

The behavior of lesser noise at coarser scale can be verified in Fig. 1. One can observe that the zoomed version of the patch extracted from the edginess feature of the coarser scale noisy image (Fig. 1 (c)) is equivalent to the same of the coarser scale clean image (Fig. 1 (b)). However, the patch extracted from the edginess feature of the noisy cameraman image is quite different from rest of the patches. Since, the patch

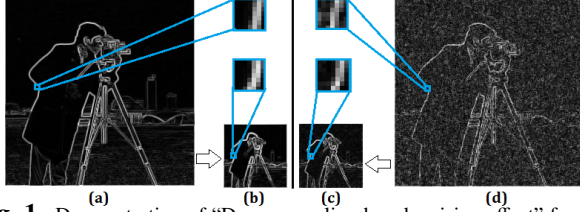


**Fig. 1.** Demonstration of “Down-sampling has denoising effect” for cameraman image: (a) the edginess feature of the clean image, (b) the edginess feature of the down-sampled (by factor 3) cameraman image, (c) the edginess feature of the down-sampled (by factor 3) noisy cameraman image (noise level  $\sigma = 50$ ), and (d) the edginess feature of the noisy cameraman image.

from (Fig. 1 (a)) is quite similar to the patch from (Fig. 1 (c)), one can judge that significant amount of noise can be reduced by going to coarser scale of the noisy image. Thus, it is logical to preserve edges in coarser scale of the image instead of the original scale.

The process of incorporating the constraint is depicted in Fig. 2. The noisy image is first denoised via an existing de-

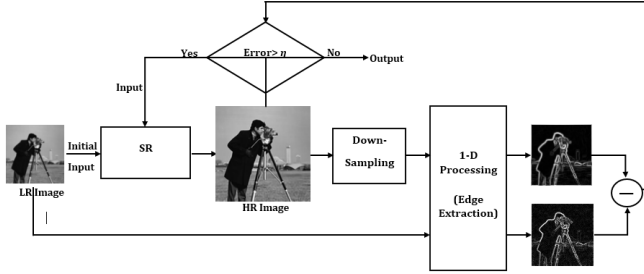


**Fig. 2.** Block diagram representation of preserving edges at coarser scales.

noising algorithm (here NCSR [10]). The denoised image is down-sampled along with the input noisy image. Edginess features are extracted from both the down-sampled versions of noisy image as well as denoised image by 1-D processing of image [11]. A large deviation between the edginess features of the down-sampled images will cause the system to iterate until convergence.

In the proposed approach, edginess feature [11] is chosen and computed using 1-D processing of images, which involves initial smoothing of image along one direction and derivative operation along orthogonal direction. This operation is repeated along two orthogonal directions and magnitude of the edges are computed using the same. Note that the computation of edginess feature does not involve any thresholding.

Let's assume that  $\mathbf{y}_l$  and  $\hat{\mathbf{x}}_l$  are produced by blurring ( $\mathbf{H}$ ) and down-sampling ( $\mathbf{D}$ ) the images  $\mathbf{y}$  and  $\hat{\mathbf{x}}$ , respectively i.e.,  $\mathbf{y}_l = \mathbf{D}\mathbf{H}\mathbf{y}$  &  $\hat{\mathbf{x}}_l = \mathbf{D}\mathbf{H}\hat{\mathbf{x}} = \mathbf{D}\mathbf{H}\mathbf{A}\hat{\mathbf{c}}$ , and  $\mathbf{E}$  is the matrix responsible for extraction of edginess feature from the image. Here, the constraint  $\|\mathbf{E}\mathbf{y}_l - \mathbf{E}\mathbf{D}\mathbf{H}\mathbf{A}\hat{\mathbf{c}}\|_2^2 \leq \varepsilon$  is added with the cost function mentioned in Eq. (4) as a regularization term

$$\hat{\mathbf{c}}_y = \arg \min_{\mathbf{c}} \left\{ \|\mathbf{y} - \mathbf{A}\mathbf{c}\|_2^2 + \lambda \sum_i \|\mathbf{c}_i - \boldsymbol{\psi}_i\|_1 + \beta \|\mathbf{E}\mathbf{y}_l - \mathbf{E}\mathbf{D}\mathbf{H}\mathbf{A}\hat{\mathbf{c}}\|_2^2 \right\}, \quad (5)$$

where,  $\beta$  is the regularization parameter. The last term of the equation enforces the edges of the noisy image to coincide with the edges of the denoised one at coarser scale.

### 3.1.1. Multi-scale edge preservation

It is important to decide a suitable down-sampling factor ( $\mathbf{D}$ ) because higher down-sampling factor can reduce noise drastically but, at the same time the edges become inconspicuous. This situation is addressed by preserving edge at different down-sampling factors with different values of  $\beta$ . Hence, the last term of eqn. (5) can be written as

$$\beta \|\mathbf{E}\mathbf{y}_l - \mathbf{E}\mathbf{D}\mathbf{H}\mathbf{A}\hat{\mathbf{c}}\|_2^2 = \sum_s \beta_s \|\mathbf{E}(\mathbf{y}) \downarrow_{d_s} - \mathbf{E}(\mathbf{A}\hat{\mathbf{c}}) \downarrow_{d_s}\|_2^2, \quad (6)$$

where,  $(\cdot) \downarrow_{d_s}$  is the down-sampling operation by factor  $d_s$ , which is equivalent to multiplication with  $\mathbf{D}\mathbf{H}$ . Here,  $s = \{1, 2, 3\}$  and  $\beta_s = \frac{1}{\sigma d_s}$  ( $\sigma =$  noise level). Thus,  $\beta$  will be assigned a lesser value with increasing either noise level or down-sampling factor. This is because, at very higher down-sampling factor or at higher strength of noise, the edges are less likely to be preserved. Hence, it is sensible to assign lesser weight to the edge preserving constraint.

### 3.2. Preventing transitional smoothing

In this case, the transitional smoothing is prevented by preserving the edge of intermediate denoising result at each iteration. The motivation behind such constraint is that most of the denoising algorithms remove noise iteratively. As a result, the image details such as edges, corners are getting blurred at each iteration, though the suppression of noise is improving. Here, the image denoising is performed by reducing sparse coding noise, which involves an approximation of  $\boldsymbol{\psi}_i$  using non-local mean of the similar patches within each iteration. Since, non-local mean is the weighted average of the non-local similar patches, employing the mean to derive  $\boldsymbol{\psi}_i$  and minimizing the sparse coding noise by eq. (4) may produce a smoother result.

In order to prevent transitional smoothing (above discussed), the second constraint is followed as shown schematically in Fig. 3, where denoising algorithm removes noise iteratively. Edginess features are extracted from the inter-

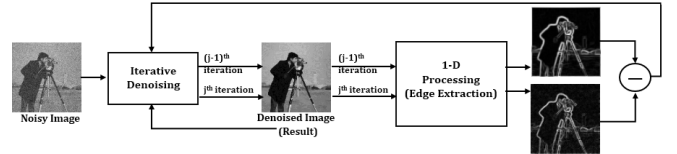


**Fig. 3.** Block diagram for preventing transitional smoothing

mediate resultant images and are examined for preservation. A large difference between the two makes the system iterate until the difference comes down within a threshold limit. The process is addressed mathematically by incorporating

the constraint  $\|\mathbf{EA}\hat{\mathbf{c}}^j - \mathbf{EA}\hat{\mathbf{c}}^{j-1}\|_2^2 \leq \xi$  in eq. (5) to preserve the edges of the intermediate results. The constraint can be incorporated with a regularization parameter  $\gamma$  as

$$\hat{\mathbf{c}}_y = \arg \min_{\mathbf{c}} \left\{ \|\mathbf{y} - \mathbf{Ac}\|_2^2 + \lambda \sum_i \|\mathbf{c}_i - \boldsymbol{\psi}_i\|_1 + \beta \|\mathbf{E}\mathbf{y}_l - \mathbf{EDHA}\hat{\mathbf{c}}\|_2^2 + \gamma \|\mathbf{EA}\hat{\mathbf{c}}^j - \mathbf{EA}\hat{\mathbf{c}}^{j-1}\|_2^2 \right\} \quad (7)$$

The eq. (7) can be solved by iterative thresholding algorithm [19]. Here, the last term attempts that the edginess feature of the intermediate result of  $j^{\text{th}}$  iteration is following the same of the intermediate result of  $(j-1)^{\text{th}}$  iteration. Thus, transitional smoothing can be prevented and a better result is expected. The algorithm of the proposed approach is depicted in Algorithm 1. Here,  $\mathbf{P}_i$  is used to extract patches

---

**Algorithm 1:** Proposed approach of image denoising

---

**Data:** Noisy image  $\mathbf{y}$

**Result:** Denoised image  $\hat{\mathbf{x}}$

```

1 Initialization:
2 Set initial approximation  $\hat{\mathbf{x}} = \mathbf{y}$ 
3 Set the regularization parameters  $\lambda, \alpha, \beta$  and  $\gamma$ .
4 Main Iteration:
5 for  $j = 1$  to  $N$ ; //  $N = \text{No. of iterations}$ 
6 do
7   Learn sub-dictionaries  $\mathbf{A}$  from  $\hat{\mathbf{x}}$  by extracting patches,
   clustering them and applying principal component analysis [10].
8    $\hat{\mathbf{x}}^{(j+1/4)} = \hat{\mathbf{x}}^{(j)} + \alpha (\mathbf{y} - \hat{\mathbf{x}}^{(j)})$ 
9   Extract Patches  $\hat{\mathbf{x}}_i^{(j+1/4)} = \mathbf{P}_i \hat{\mathbf{x}}^{(j+1/4)}$ 
10  for  $i = 1$  to  $L$ ; //  $L = \text{No. of Patches}$ 
11  do
12    Compute  $\hat{\mathbf{c}}_i^{(j+1/4)} = \mathbf{A}^T \hat{\mathbf{x}}_i^{(j+1/4)}$ 
13    Calculate  $\boldsymbol{\psi}_i = \sum_{s \in \Theta_i} \frac{1}{z} \exp\left(-\frac{\|\hat{\mathbf{x}}_i^{(j+1/4)} - \hat{\mathbf{x}}_{i,s}^{(j+1/4)}\|_2^2}{h}\right) \hat{\mathbf{c}}_i^{(j+1/4)}$ 
14    Update  $\hat{\mathbf{c}}_i^{(j+2/4)} = \text{Shrink}_{\lambda}(\hat{\mathbf{c}}_i^{(j+1/4)} - \boldsymbol{\psi}_i) + \boldsymbol{\psi}_i$ 
15    Restore a patch  $\hat{\mathbf{x}}_i^{(j+2/4)} = \mathbf{A}\hat{\mathbf{c}}_i^{(j+2/4)}$ 
16  end
17  Achieve the full image
    $\hat{\mathbf{x}}^{(j+2/4)} \approx (\sum_{i=1}^L \mathbf{P}_i^T \mathbf{P}_i)^{-1} \sum_{i=1}^L (\mathbf{P}_i^T \hat{\mathbf{x}}_i^{(j+2/4)})$ 
18  Preserving edges at coarser scales (Including  $1^{\text{st}}$  constraint)
    $\hat{\mathbf{x}}^{(j+3/4)} = \hat{\mathbf{x}}^{(j+2/4)} + \beta (\mathbf{EDH})^T (\mathbf{EDH}\mathbf{y} - \mathbf{EDH}\hat{\mathbf{x}}^{(j+2/4)})$ 
19  Preventing transitional smoothing (Including  $2^{\text{nd}}$  constraint)
    $\hat{\mathbf{x}}^{(j+1)} = \hat{\mathbf{x}}^{(j+3/4)} + \gamma \mathbf{E}^T (\mathbf{E}\hat{\mathbf{x}}^{(j+3/4)} - \mathbf{E}\hat{\mathbf{x}}^{(j)})$ 
20  if  $\|\hat{\mathbf{x}}^{j+1} - \hat{\mathbf{x}}^j\|_2^2 < \epsilon$  then
21  | break; // Breaks the loop and produce the result  $\hat{\mathbf{x}}^{j+1}$ 
22  else
23  | continue;
24  end
25 end

```

---

from image i.e.  $\mathbf{x}_i = \mathbf{P}_i \mathbf{x}$ . *Shrink* is a soft thresholding function, which is used to compute the sparse coefficient vector. Each term of eqn. (7) is solved in sequential manner to produce  $\hat{\mathbf{x}}^{(j+1/4)}$ ,  $\hat{\mathbf{x}}^{(j+2/4)}$ ,  $\hat{\mathbf{x}}^{(j+3/4)}$  &  $\hat{\mathbf{x}}^{(j+1)}$ , where  $\hat{\mathbf{x}}^{(j+1)}$  is the final result.

## 4. EXPERIMENTAL RESULTS

The performance of the proposed approach is compared with state-of-the-art approaches [8, 10, 20, 21] using standard images. The images are first added with additive white Gaussian noise of standard deviations  $\sigma = 10, 20, 50, 100$  separately to generate the noisy versions of the images. Here,  $7 \times 7$  patches are extracted from the noisy image for further processing. The denoised results are compared qualitatively as well as quantitatively. In quantitative evaluation, peak signal-to-noise ratio (PSNR) and structural similarity index (SSIM) [22] are chosen in order to evaluate the results in error perspective as well as similarity measurement. The proposed approach involves parameters  $\lambda, \alpha, \beta$  and  $\gamma$ .  $\lambda$  is chosen adaptively to get the best results, as is done in [10]. Depending on the scale-factor ( $d$ ) and the strength of noise ( $\sigma$ ), we have chosen  $\beta_s = \frac{1}{\sigma d_s}$ , where,  $s = \{1, 2, 3\}$ .  $\alpha$  and  $\gamma$  are empirically chosen as 0.02 and 5, and are kept same for all the target images.

The quantitative results are shown in Table 1, where PSNR and SSIM values are reported on top and bottom in each row, respectively. The values with bold fonts represent our best case. One can note that the proposed approach is outperforming the approaches like anisotropic TV [20], EPLL [21], K-SVD denoising [8]. In sparsity based denoising, the proposed approach and the NCSR approach are producing better than the K-SVD dictionary based denoising. This also proves that multiple compact sub-dictionaries are better than a single over-complete dictionary. However, the proposed approach is producing comparable results with the approach NCSR denoising [10]. This is because, the proposed approach focuses more on preserving the dominant (perceptually important) edges, and in turn the weak edges may be diminished with an increasing strength of noise.

Qualitative comparison of the proposed approach along with the existing approaches for two images *peppers* and *fingerprint* are shown in Figs. 4 & 5, respectively. One can observe that the anisotropic TV (ATV) is not able to remove substantial amount of noise. However, the K-SVD denoising approach is able to remove noise but, can not retain the edges efficiently. For *fingerprint* image, the ridges are overlapped with each other at some places. On the other hand, the NCSR denoising approach is able produce results of considerable quality. Nevertheless, at some areas (marked by black colored rectangular box) the NCSR denoising approach is not able to maintain the edges appropriately. Whereas, the proposed approach is able to remove noise while preserving edges, in both the examples. One can note in case of *peppers* image that the wave like pattern within black colored box are properly maintained by the proposed approach as compared to the existing approaches. Similarly, one can closely observe the regions within the black colored boxes for the *fingerprint* image to point out that the ridges are sharply preserved by the proposed approach as compared to other approaches. From

**Table 1.** Quantitative Comparison of Results Produced by Denoising Approaches via PSNR (top) & SSIM (bottom)

Approaches→	ATV [20]				EPLL [21]				K-SVD [8]				NCSR [10]				Proposed Approach			
Images↙ $\sigma$	10	20	50	100	10	20	50	100	10	20	50	100	10	20	50	100	10	20	50	100
Lena	30.22	29.86	23.02	12.47	35.56	32.60	28.42	25.30	32.28	31.23	27.78	24.49	35.81	32.92	28.89	25.66	<b>35.85</b>	<b>32.96</b>	<b>28.93</b>	25.64
	0.8222	0.8115	0.4057	0.0934	0.9126	0.8684	0.7713	0.6573	0.8608	0.8414	0.7603	0.6447	0.9149	0.8760	0.8026	0.7257	<b>0.9166</b>	<b>0.8783</b>	<b>0.8061</b>	0.7176
Barbara	24.83	24.79	21.61	12.37	33.59	29.75	24.83	22.10	30.59	29.42	25.43	21.87	34.98	31.72	27.10	23.30	34.96	<b>31.72</b>	27.05	<b>23.32</b>
	0.7057	0.7030	0.4407	0.1421	0.9319	0.8744	0.7031	0.5441	0.8757	0.8471	0.7128	0.5335	0.9411	0.9045	0.7962	0.6498	<b>0.9417</b>	<b>0.9048</b>	0.7923	0.6455
Couple	27.68	27.49	22.46	12.43	33.78	30.47	26.22	23.34	29.89	28.73	25.25	22.61	33.94	30.56	26.21	23.22	<b>33.98</b>	<b>30.58</b>	26.12	23.11
	0.7350	0.7316	0.4536	0.1270	0.9077	0.8364	0.6883	0.5380	0.8110	0.7739	0.6318	0.5012	0.9064	0.8363	0.6925	0.5554	<b>0.9084</b>	<b>0.8394</b>	<b>0.6927</b>	0.5532
Fingerprint	24.56	24.34	21.08	12.36	32.13	28.29	23.58	19.80	28.30	27.05	23.07	18.33	32.70	28.99	24.53	21.29	32.65	28.96	24.50	<b>21.34</b>
	0.8211	0.8185	0.7108	0.3289	0.9678	0.9262	0.8022	0.5877	0.9188	0.8920	0.7456	0.4406	0.9704	0.9327	0.8260	0.6816	0.9698	0.9312	0.8241	<b>0.6840</b>
Hill	28.55	28.36	22.78	12.45	33.49	30.47	26.91	24.37	30.04	29.08	26.25	24.01	33.69	30.61	26.86	24.13	<b>33.69</b>	<b>30.65</b>	<b>26.91</b>	<b>24.31</b>
	0.7131	0.7097	0.4214	0.0973	0.8859	0.7983	0.6597	0.5381	0.7715	0.7349	0.6193	0.5269	0.8864	0.8013	0.6586	0.5541	<b>0.8869</b>	<b>0.8036</b>	<b>0.6611</b>	<b>0.5561</b>
Man	28.43	28.22	22.71	12.44	33.90	30.53	26.63	23.96	29.97	28.93	26.03	23.40	33.96	30.52	26.60	23.97	<b>34.01</b>	<b>30.56</b>	<b>26.61</b>	23.91
	0.7542	0.7498	0.4332	0.1093	0.9093	0.8347	0.6943	0.5690	0.8083	0.7730	0.6628	0.5493	0.9069	0.8311	0.6976	0.6022	<b>0.9086</b>	<b>0.8325</b>	<b>0.6985</b>	0.5975
Peppers	28.89	28.43	22.38	12.37	34.51	31.18	26.60	22.93	30.57	29.43	26.08	21.69	34.66	31.26	26.53	22.64	34.65	31.24	<b>26.63</b>	<b>22.78</b>
	0.8450	0.8296	0.4698	0.1414	0.9273	0.8854	0.7847	0.6595	0.8700	0.8491	0.7662	0.6118	0.9262	0.8861	0.7969	0.6958	<b>0.9262</b>	0.8847	0.7958	0.6895
Average	27.59	27.35	22.29	12.41	33.85	30.47	26.17	23.11	30.23	29.12	25.70	22.34	34.25	30.94	26.67	23.45	<b>34.26</b>	<b>30.95</b>	<b>26.68</b>	<b>23.49</b>
	0.7709	0.7648	0.4765	0.1484	0.9204	0.8605	0.7291	0.5848	0.8452	0.8159	0.6998	0.5440	0.9217	0.8668	0.7529	0.6378	<b>0.9226</b>	<b>0.8678</b>	<b>0.7529</b>	0.6348

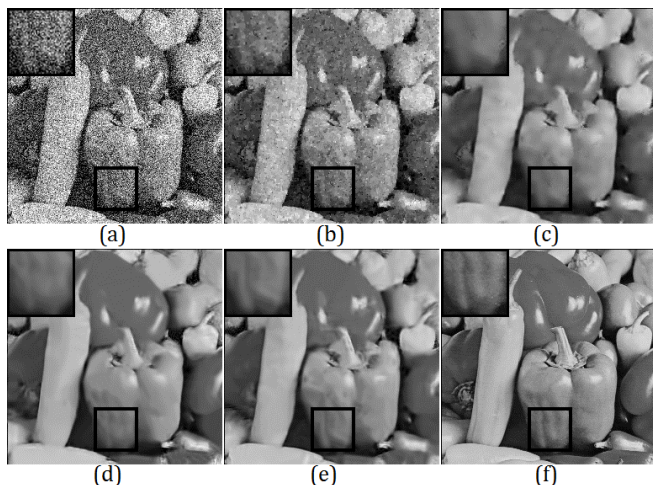


**Fig. 4.** Comparison of denoising results for noisy Pepper image ( $\sigma = 50$ ): (a) The noisy image (PSNR=14.12), (b) the result of ATV [20] (PSNR=22.38), (c) the result of K-SVD denoising [8] (PSNR=26.08), (d) the result of NCSR [10] (PSNR=26.53), (e) the result of the proposed approach (PSNR=26.63), and (f) the ground truth image.

the above observations, it can be inferred that the proposed approach is able to maintain the strong edges while removing noise as compared to the state-of-the-art approaches.

## 5. SUMMARY

In this paper, we have attempted to preserve edges of images while removing noise using two constraints. The first constraint aims to make edges of the noisy image consistent with the denoised image at the coarser scale. It has been done based on the observation that the strong edges are less effected while the level of noise comes down drastically at the coarser scale. The approach is made more robust by preserving the edges at different down-sampling factors to account the dif-

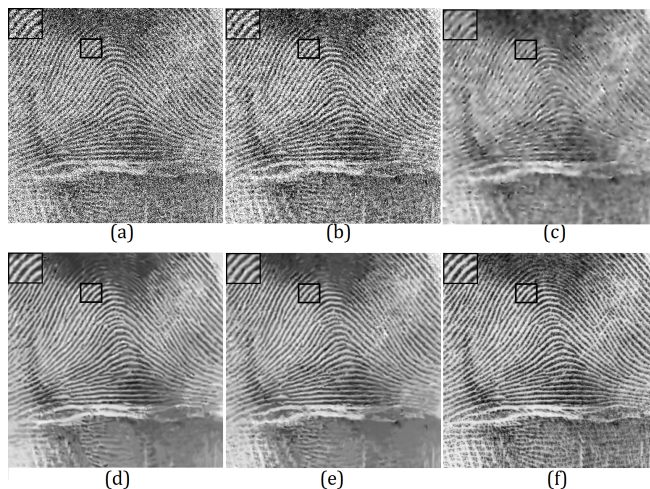


**Fig. 5.** Comparison of denoising results for noisy fingerprint image ( $\sigma = 100$ ): (a) The noisy image (PSNR=8.12), (b) the result of ATV [20] (PSNR=12.36), (c) the result of K-SVD denoising [8] (PSNR=18.33), (d) the result of NCSR [10] (PSNR=21.29), (e) the result of the proposed approach (PSNR=21.34), and (f) the ground truth image.

ferent strength of noises. The second constraint has been included by preserving edges of the intermediate results of each iteration in order to prevent transitional smoothing of images. The proposed constraints can be applied to any denoising approach to preserve strong edges while removing noise.

## 6. REFERENCES

- [1] Antoni Buades, Bartomeu Coll, and Jean-Michel Morel, “A review of image denoising algorithms, with a new one,” *Multiscale Modeling & Simulation*, vol. 4, no. 2, pp. 490–530, 2005.
- [2] P. Perona and J. Malik, “Scale-space and edge detection

- using anisotropic diffusion,” *IEEE Transactions on Pattern Analysis and Machine Intelligence*, vol. 12, no. 7, pp. 629–639, Jul 1990.
- [3] Leonid I. Rudin, Stanley Osher, and Emad Fatemi, “Nonlinear total variation based noise removal algorithms,” *Physica D: Nonlinear Phenomena*, vol. 60, no. 14, pp. 259 – 268, 1992.
- [4] A. Levin, Y. Weiss, F. Durand, and W.T. Freeman, “Efficient marginal likelihood optimization in blind deconvolution,” in *IEEE Conference on Computer Vision and Pattern Recognition (CVPR), 2011*, June 2011, pp. 2657–2664.
- [5] Vladimir Katkovnik, Alessandro Foi, Karen Egiazarian, and Jaakko Astola, “From local kernel to nonlocal multiple-model image denoising,” *International Journal of Computer Vision*, vol. 86, no. 1, pp. 1–32, 2010.
- [6] J. Mairal, F. Bach, J. Ponce, G. Sapiro, and A. Zisserman, “Non-local sparse models for image restoration,” in *IEEE 12th International Conference on Computer Vision, 2009*, Sept 2009, pp. 2272–2279.
- [7] D. Zoran and Y. Weiss, “From learning models of natural image patches to whole image restoration,” in *IEEE International Conference on Computer Vision (ICCV), 2011*, Nov 2011, pp. 479–486.
- [8] M. Elad and M. Aharon, “Image denoising via sparse and redundant representations over learned dictionaries,” *IEEE Transactions on Image Processing*, vol. 15, no. 12, pp. 3736–3745, dec. 2006.
- [9] Jeremias Sulam and Michael Elad, “Expected patch log likelihood with a sparse prior,” in *Energy Minimization Methods in Computer Vision and Pattern Recognition*, vol. 8932, pp. 99–111. 2015.
- [10] Weisheng Dong, Lei Zhang, Guangming Shi, and Xin Li, “Nonlocally centralized sparse representation for image restoration,” *IEEE Transactions on Image Processing*, vol. 22, no. 4, pp. 1620–1630, April 2013.
- [11] Anil Kumar Sao, B. Yegnanarayana, and B.V.K. Vijaya Kumar, “Significance of image representation for face verification,” *Signal, Image and Video Processing*, vol. 1, pp. 225–237, 2007.
- [12] M. Zontak, I. Mosseri, and M. Irani, “Separating signal from noise using patch recurrence across scales,” in *IEEE Conference on Computer Vision and Pattern Recognition (CVPR), 2013*, June 2013, pp. 1195–1202.
- [13] Jianchao Yang, J. Wright, T. Huang, and Yi Ma, “Image super-resolution as sparse representation of raw image patches,” in *IEEE Conference on Computer Vision and Pattern Recognition, 2008. CVPR 2008.*, june 2008, pp. 1–8.
- [14] Weisheng Dong, Lei Zhang, Guangming Shi, and Xiaolin Wu, “Image deblurring and super-resolution by adaptive sparse domain selection and adaptive regularization,” *IEEE Transactions on Image Processing*, vol. 20, no. 7, pp. 1838–1857, Jul. 2011.
- [15] S. Mandal and A.K. Sao, “Edge preserving single image super resolution in sparse environment,” in *20th IEEE International Conference on Image Processing (ICIP), 2013*, Sept 2013, pp. 967–971.
- [16] S. Mandal, A. Bhavsar, and A.K. Sao, “Hierarchical example-based range-image super-resolution with edge-preservation,” in *IEEE International Conference on Image Processing (ICIP), 2014*, Oct 2014, pp. 3867–3871.
- [17] Roman Zeyde, Michael Elad, and Matan Protter, “On single image scale-up using sparse-representations,” in *Curves and Surfaces*, vol. 6920, pp. 711–730. Springer, 2012.
- [18] S. Mandal, A. Bhavsar, and A.K. Sao, “Super-resolving a single intensity/range image via non-local means and sparse representation,” in *Indian Conference on Computer Vision, Graphics and Image Processing (ICVGIP), 2014*, Dec 2014, pp. 1–8.
- [19] I. Daubechies, M. Defrise, and C. De Mol, “An iterative thresholding algorithm for linear inverse problems with a sparsity constraint,” *Communications on Pure and Applied Mathematics*, vol. 57, no. 11, pp. 1413–1457, 2004.
- [20] Tom Goldstein and Stanley Osher, “The split bregman method for l1-regularized problems,” *SIAM Journal on Imaging Sciences*, vol. 2, no. 2, pp. 323–343, 2009.
- [21] D. Zoran and Y. Weiss, “From learning models of natural image patches to whole image restoration,” in *IEEE International Conference on Computer Vision (ICCV), 2011*, Nov 2011, pp. 479–486.
- [22] Zhou Wang, A.C. Bovik, H.R. Sheikh, and E.P. Simoncelli, “Image quality assessment: from error visibility to structural similarity,” *IEEE Transactions on Image Processing*, vol. 13, no. 4, pp. 600–612, April 2004.